



Characteristics of a supersonic laminar boundary layer over a rough wall  
by Joseph Michael DSa

A thesis submitted in partial fulfillment of the requirements for the degree of MASTER OF SCIENCE  
in Mechanical Engineering  
Montana State University  
© Copyright by Joseph Michael DSa (1982)

**Abstract:**

The characteristics of a supersonic laminar boundary layer over a rough wall were investigated. The boundary layer was produced by, a slender body of revolution at Mach 3 and the roughness consisted of random distributed and two dimensional periodic overlays. Results reported here cover mean flow profiles needed to validate and characterize the flow and detect changes in the profile caused by roughness. The critical roughness needed to cause profile distortions is based on the Reynolds number defined by local properties rather than free stream properties. The height of the distributed roughness needed to cause profile distortions caused great difficulty in interpreting the profile data. The two dimensional periodic overlay with a roughness height greater than the critical roughness height caused an upstream movement of transition. The two dimensional overlay also caused an outward displacement of the boundary layer edge with a simultaneous decrease in the boundary layer thickness causing a distinct distortion of the boundary layer profile and an increase in the surface skin friction.

STATEMENT OF PERMISSION TO COPY

In presenting this thesis in partial fulfillment of the requirements for an advanced degree at Montana State University, I agree that the Library shall make it freely available for inspection. I further agree that permission for extensive copying of this thesis for scholarly purposes may be granted by my major professor, or, in his absence, by the Director of Libraries. It is understood that any copying or publication of this thesis for financial gain shall not be allowed without my written permission.

Signature \_\_\_\_\_

A handwritten signature in dark ink, appearing to be 'J. S. ...', written over a horizontal line.

Date \_\_\_\_\_

9<sup>th</sup> AUGUST 82

CHARACTERISTICS OF A SUPERSONIC LAMINAR  
BOUNDARY LAYER OVER A ROUGH WALL

by

JOSEPH MICHAEL D'SA

A thesis submitted in partial fulfillment  
of the requirements for the degree

of

MASTER OF SCIENCE

in

Mechanical Engineering

Approved:

*A. Semetko*

Chairperson, Graduate Committee

*Dennis O. Blacketter*

Head, Major Department

*Michael P. Malone*

Graduate Dean

MONTANA STATE UNIVERSITY  
Bozeman, Montana

July, 1982

**ACKNOWLEDGEMENT**

The author offers his sincere appreciation to the following for their contribution to this investigation.

His advisor, Anthony Demetriades, for his guidance and support throughout this investigation.

Bill Martindale and Bob Warrington for serving as committee members and reviewing this thesis.

Gordon Williamson for helpful assistance in constructing the models for the experiment.

John Rompel for his expertise and assistance in putting together the electronic system for the experiment.

Glenn McCullough and Mel Roush for their assistance during the course of the experiment.

The Mechanical Engineering Department of Montana State University and Air Force Office of Scientific Research for financial assistance and funding for this investigation.

Roberta Coppock for typing this thesis.

And last but not the least, his wife, Ela, for her never-ending encouragement and understanding during this investigation.

## TABLE OF CONTENTS

| <u>Chapter</u>   | <u>Page</u> |
|--|-------------|
| VITA . . . . .   | ii          |
| ACKNOWLEDGEMENT. . . . .   | iii         |
| LIST OF FIGURES. . . . .   | vi          |
| NOMENCLATURE . . . . .   | x           |
| ABSTRACT . . . . .   | xii         |
| I. INTRODUCTION . . . . .  | 1           |
| II. DESIGN OF THE EXPERIMENT. . . . .                              | 4           |
| III. DESCRIPTION OF THE MODEL AND WIND TUNNEL . . . . .            | 6           |
| IV. INSTRUMENTATION . . . . .                                      | 12          |
| V. DESCRIPTION OF MEASUREMENTS . . . . .                           | 15          |
| Transition Measurement . . . . .                                   | 15          |
| Test Matrix . . . . .  | 17          |
| Measurement of Surface Static Pressure . . . . .                   | 20          |
| Reynolds Number Corrections to the Pitot<br>Probe . . . . .        | 22          |
| Measurement of the Location of the Roughened<br>Surfaces . . . . . | 23          |
| Data Acquisition Procedures . . . . .                              | 24          |
| VI. SUMMARY ON THE RANDOM SURFACE ROUGHNESS MODEL . . . . .        | 30          |
| VII. COMPARISON OF SMOOTH AND SCREW MODEL. . . . .                 | 32          |
| VIII. CONCLUSIONS . . . . .  | 79          |
| BIBLIOGRAPHY . . . . .   | 81          |

|                        | <u>Page</u> |
|------------------------|-------------|
| APPENDICES . . . . .   | 83          |
| APPENDIX I . . . . .   | 84          |
| APPENDIX II. . . . .   | 89          |
| APPENDIX III . . . . . | 92          |
| APPENDIX IV. . . . .   | 103         |

## LIST OF FIGURES

| <u>Figure</u>   | <u>Page</u> |
|---|-------------|
| 1. Placement of the Model and Probe in the Test Section (to scale) . . . . .  | 7           |
| 2. Top: Exploded View of Model and Roughness Afterbodies. Bottom: Wind-Tunnel Installation . .                            | 8           |
| 3. Views of the Model in the Tunnel. Note Microscope for Probe-Tip Observation . . . . .                                  | 9           |
| 4. Details of Probe-Tip and Measuring Circuit. . . . .  | 13          |
| 5. Microphotographs of Roughness Profiles for Screw-Type Model (top) and 60-Grit or $k = 0.004''$ Model (below) . . . . . | 19          |
| 6. Static Pressure and Mach Number (From Static and Pitot Pressure) Results for Smooth Model. . . . .                     | 34          |
| 7. Static Pressure and Mach Number (From Static and Pitot Pressure) Results for Screw Model . . . . .                     | 35          |
| 8. Static Pressure Surveys . . . . .  | 36          |
| 9. Mach Number Results (From Static Pressure and Supply Pressure) . . . . .   | 37          |
| 10. Velocity Profile on Smooth Wall, $x = 6''$ , $P_0 = 600$ millimeters Hg (Mercury). . . . .                            | 38          |
| 11. Velocity Profile on Smooth Wall, $x = 4''$ , $P_0 = 400$ mm. Hg . . . . .   | 39          |
| 12. Velocity Profile on Smooth Wall, $x = 4$ , $P_0 = 500$ mm. Hg . . . . .   | 40          |
| 13. Velocity Profile on Smooth Wall, $x = 4''$ , $P_0 = 600$ mm. Hg . . . . .   | 41          |
| 14. Linearity of Velocity Variation Near Wall for Smooth Model, $x = 6''$ , $P_0 = 400$ mm. Hg . . . . .                  | 42          |

| <u>Figure</u>   | <u>Page</u> |
|---|-------------|
| 15. Linearity of Velocity Variation Near Wall for Smooth Model, $x = 6''$ , $P_0 = 500$ mm. Hg . . . . .              | 43          |
| 16. Velocity Profile on Screw Model, $x = 5''$ , $P_0 = 400$ mm. Hg (Note Pitot Probe). . . . .                       | 45          |
| 17. Velocity Profile on Screw Model, $x = 4''$ , $P_0 = 400$ mm. Hg . . . . .   | 46          |
| 18. Velocity Profile on Screw Model, $x = 7''$ , $P_0 = 500$ mm. Hg . . . . .   | 47          |
| 19. Velocity Profile on Screw Model, $x = 6''$ , $P_0 = 500$ mm. Hg . . . . .   | 48          |
| 20. Velocity Profile on Screw Model, $x = 6''$ , $P_0 = 400$ mm. Hg . . . . .   | 49          |
| 21. Pitot Pressure Profile on Screw Model, $x = 4''$ , $P_0 = 600$ mm. Hg . . . . .                                   | 51          |
| 22. Comparison Between Smooth and Screw Velocity Profiles, $x = 6''$ , $P_0 = 400$ mm. Hg . . . . .                   | 52          |
| 23. Comparison Between Smooth and Screw Velocity Profiles, $x = 6''$ , $P_0 = 500$ mm. Hg . . . . .                   | 53          |
| 24. Comparison Between Smooth and Screw Velocity Profiles, $x = 6''$ , $P_0 = 600$ mm. Hg . . . . .                   | 54          |
| 25. Comparison Between Smooth and Screw Velocity Profiles, $x = 7''$ , $P_0 = 600$ mm. Hg . . . . .                   | 55          |
| 26. Comparison Between Smooth and Screw Velocity Profiles, $x = 7''$ , $P_0 = 400$ mm. Hg . . . . .                   | 56          |
| 27. Temperature Profile on Smooth Model, $x = 4''$ , $P_0 = 500$ mm. Hg. Note Surface Datum (Square on Axis). . . . . | 57          |
| 28. Temperature Profile on Smooth Model for $x = 4''$ , $P_0 = 600$ mm. Hg. Note Datum (Square on Axis) . . . . .     | 58          |



| <u>Figure</u>  | <u>Page</u> |
|--|-------------|
| 29. a. Determination of "Virtual Origin" for Smooth Model ( $\delta^2$ vs. $x$ ) . . . . .   | 60          |
| b. Determination of "Virtual Origin" for Smooth Model ( $\theta^2$ vs. $x$ ) . . . . .   | 61          |
| 30. a. Determination of "Virtual Origin" for Screw Model ( $\delta^2$ vs. $x$ ) . . . . .  | 62          |
| b. Determination of "Virtual Origin" for Screw Model ( $\theta^2$ vs. $x$ ) . . . . .  | 63          |
| 31. Form Factor for Smooth and Screw Model. . . . .  | 64          |
| 32. a. Momentum Thickness and Unit Reynolds Number Results for Smooth Model. . . . .   | 65          |
| b. Momentum Reynolds Number Results for Smooth Model . . . . .   | 66          |
| c. Boundary Layer Thickness Results for Smooth Model . . . . .   | 67          |
| 33. a. Momentum Thickness and Unit Reynolds Number Results for Screw Model . . . . .   | 68          |
| b. Momentum Reynolds Number Results for Screw Model . . . . .  | 69          |
| c. Boundary Layer Thickness Results for Screw Model . . . . .  | 70          |
| 34. Schlieren Photograph of Screw Model ( $P_0 = 600$ mm. Hg). Note Onset of Transition . . . . .                                  | 72          |
| 35. Skin Friction Results for Smooth Model. . . . .  | 73          |
| 36. Third Degree Polynomial Fit of Velocity Variation Near Effective Screw Surface, $x = 4''$ , $P_0 = 400$ mm. Hg. . . . .        | 75          |
| 37. Third Degree Polynomial Curve Fit of Velocity Variation Near Effective Screw Surface, $x = 4''$ , $P_0 = 500$ mm. Hg . . . . . | 76          |

| <u>Figure</u>  | <u>Page</u> |
|--|-------------|
| 38. Third Degree Polynomial Curve Fit of Velocity<br>Variation Near Effective Screw Surface, $x = 5''$<br>$P_0 = 600$ mm. Hg . . . . . | 77          |
| 39. Skin Friction Results for Screw Model . . . . .  | 78          |

## NOMENCLATURE

| <u>Symbol</u> | <u>Description</u>  |
|---------------|---|
| $c_{f1}$ :    | Friction coefficient (wall viscosity)   |
| $c_{f2}$ :    | Friction coefficient (stream viscosity)   |
| $k$ :         | Roughness height  |
| $k_1$ :       | Critical height for destabilization/transition  |
| $M$ :         | Mach number   |
| $P$ :         | Pressure  |
| $P_T$ :       | Pitot pressure reading  |
| $R$ :         | Gas constant  |
| $Re'$ :       | Unit Reynolds number  |
| $Re_\theta$ : | Momentum Reynolds number  |
| $Re_{e,T}$ :  | Critical Reynolds number for destabilization<br>(based on roughness height and stream properties)         |
| $Re_k$ :      | Critical Reynolds number for destabilization<br>(based on roughness height and conditions at that height) |
| $T$ :         | Temperature   |
| $T_{op}$ :    | Local stagnation temperature at pitot tube  |
| $u$ :         | Velocity  |
| $x$ :         | Axial Coordinate (measured from trailing edge forward)  |
| $y$ :         | Coordinate normal to the surface  |
| $\tilde{y}$ : | Transformed coordinate normal to the surface  |

| <u>Symbol</u>      | <u>Description</u>             |
|--------------------|--------------------------------|
| $\gamma$ :         | Specific heat ratio            |
| $\delta$ :         | Boundary layer thickness       |
| $\delta^*$ :       | Displacement thickness         |
| $\theta$ :         | Momentum thickness             |
| $\mu$ :            | Viscosity                      |
| $\nu$ :            | Kinematic Viscosity            |
| $\rho$ :           | Density                        |
| ( ) <sub>o</sub> : | Stagnation (supply) conditions |
| ( ) <sub>e</sub> : | Boundary-Layer edge conditions |
| ( ) <sub>k</sub> : | Conditions at roughness height |
| ( ) <sub>w</sub> : | Conditions on wall surface     |

ABSTRACT

The characteristics of a supersonic laminar boundary layer over a rough wall were investigated. The boundary layer was produced by a slender body of revolution at Mach 3 and the roughness consisted of random distributed and two dimensional periodic overlays. Results reported here cover mean flow profiles needed to validate and characterize the flow and detect changes in the profile caused by roughness. The critical roughness needed to cause profile distortions is based on the Reynolds number defined by local properties rather than free stream properties. The height of the distributed roughness needed to cause profile distortions caused great difficulty in interpreting the profile data. The two dimensional periodic overlay with a roughness height greater than the critical roughness height caused an upstream movement of transition. The two dimensional overlay also caused an outward displacement of the boundary layer edge with a simultaneous decrease in the boundary layer thickness causing a distinct distortion of the boundary layer profile and an increase in the surface skin friction.

## CHAPTER I

### INTRODUCTION

The purpose of the present investigation was to determine the characteristics of a supersonic laminar boundary layer over a rough wall.

There are a number of factors such as pressure gradient, surface heat transfer, bluntness, curvature and roughness that could affect the characteristics of a laminar boundary layer. The question of how roughness affects transition of a laminar boundary layer has been addressed by many researchers in the past. For instance, van Driest with McCauley (1) and later with Blumer (2) investigated the effects of three dimensional roughness on transition of supersonic laminar boundary layers, while Whitfield and Iannuzzi (3) investigated similar effects up to a Mach number of 12 to verify the hypersonic extensions of these effects proposed by Potter and Whitfield (4). Roughness, for all the above researchers, consisted of spheres glued to a smooth surface in an array. Only recently, Reshotko and Leventhal (5) and Kendall (6) worked with distributed random roughness (sandpaper) to study disturbances caused by roughness in laminar low speed boundary layers. The question of how random distributed or two dimensional periodic roughness affects characteristics

of a supersonic laminar boundary layer has been given little attention in the past.

There were three questions which were of considerable importance to the present investigation. First of all, it was necessary to determine the critical size of roughness that would show profile distortions compared to the profiles of the smooth (no roughness) surface. Second, how does roughness (above the critical size) affect the point of transition? And third, why does surface skin friction have to be greater for a rough (roughness above critical value) surface compared to a smooth surface?

The question concerning the critical size of roughness has been addressed in the past for low speed flows. According to Fiencht (7), the critical Reynolds number necessary to show profile distortions is defined by free stream properties as

$$Re_{e,T} = \frac{u_e k}{\nu_e} = 120.$$

On the other hand, Reshotko (5) and Kendall (6) motivated by Smith and Clutter (8) state that the critical Reynolds number is defined by local properties as

$$Re_k = \frac{u_k k}{\nu_e} = 100.$$

Thus it was necessary to determine which of the two Reynolds numbers is applicable for laminar supersonic

flows.

The question of why skin friction increases for a rough (roughness greater than the critical value) surface compared to a smooth surface in a supersonic laminar boundary layer has been given little attention in the past.

Although results on how roughness affects the point of transition for three dimensional roughness in laminar supersonic boundary layers have been reported (1), none have been reported for random distributed or two dimensional periodic roughness for similar boundary layers.



## CHAPTER II

### DESIGN OF THE EXPERIMENT

The criteria to be met in designing this experiment were as follows:

- a) The external condition had to be uniform and the ratio of the roughness height  $k$  to the boundary layer thickness be constant (or nearly so) over the measured length of the model so that the profile distortion be constant.
- b) The range of the Reynolds number  $Re_\theta$  had to lie below the transition value (thought to be 400-800) and yet be high enough to detect profile distortions.
- c) The ratio of  $k/\delta$  had to be large enough to detect profile distortions compared to the smooth wall case.

The test model was a sharp nosed body of revolution. In this way, the cylindrical surface, unlike a flat surface, would be void of side wall interference. The sharp nose would suppress any bluntness phenomena (e.g. entropy gradients) and the small ogive angle would not allow a large pressure drop across the weak shock from the nose. Calculations show that a model like the one mentioned when placed in the test section of the wind tunnel would have a boundary layer thick enough to avoid resolution problems with miniaturized sensors and yet thin

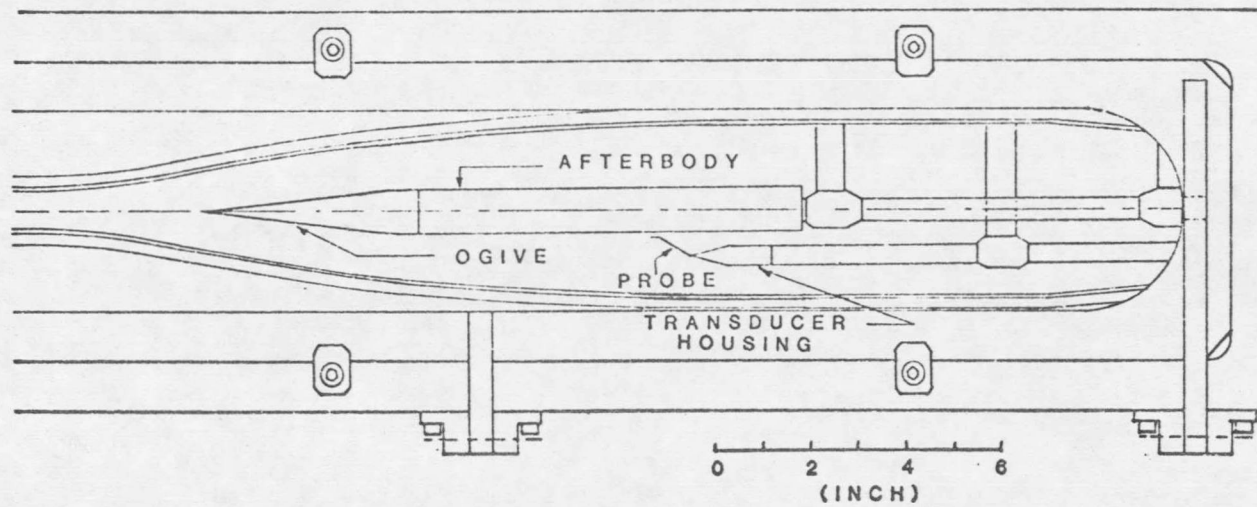
enough to avoid phenomena peculiar to axisymmetric boundary layers (9).

### CHAPTER III

#### DESCRIPTION OF MODEL AND WIND-TUNNEL

The wind-tunnel and model are pictured on Figures 1 through 3. The MSU Supersonic Wind Tunnel (MSU/SWT) is configured to operate continuously with Mach 3.0 nozzle discharging into a 3.1" x 3.2" (7.87 cm. x 8.13 cm.) test section. The stream unit Reynolds number  $Re'$  range varies from about 20,000 to 60,000 per cm.

The model consisted of a sharp ogive-cylinder combination with an overall length of 12.6" (32.0 cm). The ogive tip formed a cone  $5.2^\circ$  in half angle, with the purpose of avoiding significant shock waves reflecting on the model surface by sidewall reflection. The ogive was 4.6" (11.68 cm.) long and was detachable from the 8" (20.32 cm.) long cylindrical afterbody. Several afterbodies had been built, and the design allowed for rapid disassembly and reinstallation of the desired afterbody in the SWT without removing the entire model. The ogive-afterbody junction was designed to be flush for each afterbody choice. The entire model was suspended by two vertical actuator struts, while two additional struts supported the sensor probe in use. The model-probe arrangement could be moved vertically in unison (for example, when starting the tunnel, they were moved to the tunnel ceiling to prevent



7

Figure 1 Placement of the Model and Probe in the Test Section (to scale)















































































































































































































































